Preferential Regional Distribution of Atrial Fibrosis in Posterior Wall Around Left Inferior Pulmonary Vein as Identified by LGE-CMR in Patients with Atrial Fibrillation

Eva Benito, MD[a] * Nuno Cabanelas, MD[a] *; Marta Nuñez-Garcia, MSc[b]; Francisco Alarcón, MSc[a]; Rosa M. Figueras i Ventura, PhD[a]; David Soto-Iglesias, PhD[a;] Eduard Guasch, MD, PhD[a,c]; Susanna Prat-Gonzalez, MD, PhD[a]; Rosario J. Perea, MD, PhD[a]; Roger Borràs, BSc[a]; Constantine Butakoff, PhD[b]; Oscar Camara, PhD[b]; Felipe Bisbal, MD, PhD[c,d]; Elena Arbelo MD, PhD[a,c]; José Maria Tolosana MD, PhD[a,c]; Josep Brugada MD, PhD[a,c]; Antonio Berruezo, MD, PhD[a,c] and Lluís Mont MD, PhD[a,c]

[a] *Department of Cardiology, Unitat de Fibril.lació Auricular (UFA), Hospital Clinic, Universitat de Barcelona, Barcelona, Catalonia, Spain. Institut d'Investigacions Biomèdiques August Pi i Sunyer (IDIBAPS), Barcelona, Catalonia, Spain*

[b] *PhySense, Department of Information and Comunication Technologies (DTIC) Universitat Pompeu Fabra, Barcelona, Catalonia, Spain*

[c] *CIBER de Enfermedades Cardiovasculares*

[d] *Heart Institute (iCOR), Hospital Universitari Germans Trias i Pujol. Barcelona, Catalonia Spain*

*The first 2 authors (EB and NC) have equally contributed to the study

Conflict of interest: None reported

Short title: Regional distribution of LA fibrosis in AF

Word Count: 4488

Authors email addresses: Benitom@clinic.cat; ncabanelas@gmail.com; marta.nunez@upf.edu; falarcon@clinic.cat; Rfigueras@clinic.cat; dsoto@clinic.cat ; eguasch@clinic.cat; Suprat@clinic.cat; Rjperea@clinic.cat; Rborras@clinic.cat; constantine.butakoff@upf.edu; oscar.camara@upf.edu; f.bisbalvb@gmail.com; Earbelo@clinic.cat; Tolosana@clinic.cat; Jbrugada@clinic.cat; Berruezo@clinic.cat; Lmont@clinic.cat

Correspondence should be sent:

Dr. J. Lluís Mont Girbau
lmont@clinic.cat
Cardiology Department, Hospital Clinic
C/ Villarroel Nº 170. 08036 Barcelona
Tel: (+34) 932275551; Fax: (+34) 934513045

ABSTRACT

Aims: Left atrial (LA) fibrosis can be identified by late gadolinium enhancement cardiac magnetic resonance (LGE-CMR) in patients with atrial fibrillation (AF). However, there is limited information about anatomical fibrosis distribution in the left atrium. The aim is to determine whether there is a preferential spatial distribution of fibrosis in the left atrium in patients with AF.

Methods: A 3Tesla LGE-CMR was performed in 113 consecutive patients referred for AF ablation. Images were post-processed and analyzed using ADAS-AF software (Galgo Medical), which allows fibrosis identification in 3-dimensional color-coded shells. A regional semiautomatic LA parcellation software was used to divide the atrial wall into 12 segments: 1-4, posterior wall; 5-6, floor; 7, septal wall; 8-11, anterior wall; 12, lateral wall. The presence and amount of fibrosis in each segment was obtained for analysis.

Results: After exclusions for artifacts and insufficient image quality, 76 LGE-MRI images (68%) were suitable for fibrosis analysis. Segments 3 and 5, closest to the left inferior pulmonary vein, had significantly higher fibrosis (40.42%±23.96 and 25.82%±21.24, respectively; $p<0.001$), compared to other segments. Segments 8 and 10 in the anterior wall contained the lowest fibrosis (2.54%±5.78 and 3.82%±11.59, respectively; $p<0.001$). Age >60 years was significantly associated with increased LA fibrosis (95%CI 0.19 to 8.39, $p=0.04$) and persistent AF approached significance (95%CI -0.19% to 7.83%, $p=0.08$).

Conclusion: In patients with AF, the fibrotic area is preferentially located at the posterior wall and floor around the antrum of the left inferior pulmonary vein. Age >60 years was associated with increased fibrosis.

KEY WORDS:

Atrial fibrillation; fibrosis; LGE-CMR; regional distribution; risk factors.

CONDENSED ABSTRACT

113 3T LGE-CMR of patients with AF were acquired previous to the ablation procedure. The left atrial fibrosis showed a significant preferential distribution in the posterior wall and floor close to the left inferior pulmonary vein. Age>60 years and persistent AF type were associated with higher percentage of fibrosis.

INTRODUCTION

The electrophysiological mechanisms that sustain atrial fibrillation (AF) are not fully understood. The main hypothesis is that a combination of focal firing from triggered activity and atrial remodeling facilitate re-entry,[1] creating the underlying conditions for AF. This remodelling is the result of structural and functional adaptive changes produced in the atrial wall, and is a key factor in the onset, progression, and maintenance of AF.[2]

Atrial fibrosis is part of the remodeling process as a response to inflammation, stretch or overload imposed by risk factors or by aging.[3, 4] In animal models, atrial fibrosis increases the predisposition to AF.[5] In addition, persistency of AF is a major determinant for increased tissue remodeling and fibrosis.[6] In a histological analysis of tissue samples obtained from patients with advanced structural disease, the areas more affected by interstitial remodeling in persistent AF were located in the left atrial wall around the pulmonary vein (PV) ostia.[7]

In recent years, late gadolinium enhancement cardiac magnetic resonance (LGE-CMR) imaging has been recognized as a useful diagnostic and prognostic tool in noninvasive assessment of atrial myocardial fibrosis of patients with AF.[8-10] Fibrosis identified by LGE-CMR shows a correlation with areas of low voltage in electroanatomic mapping.[9]

The aim of the present study was to determine if there is a preferential regional distribution of fibrosis in the left atrium, as assessed by LGE-CMR in patients with AF, and to identify any preferentially affected regions.

METHODS

Sample Population

A cohort of 113 consecutive patients with AF referred for a first ablation procedure under current guidelines[11] between May 2011 and March of 2015 and assessed by 3Tesla LGE-CMR, obtained <7 days pre-ablation, were included. Baseline clinical and echocardiographic characteristics also were collected before the ablation procedure.

The study was an observational prospective collection of clinical and LGE-CMR data in patients undergoing AF ablation. The protocol was reviewed and approved by the Hospital Clinic Ethics Committee. An informed consent was obtained from all patients.

Image acquisition and late gadolinium enhancement cardiac magnetic resonance post-processing

LGE-CMR image acquisition

All LGE-CMR images were obtained <7 days prior to the ablation procedure. To guarantee good image quality, all were acquired in sinus rhythm and cardioversion was performed before the study when necessary. The acquisition protocol has been previously reported.[12] and is extensively described in Supplementary Material. Briefly, 3D-LGE images were acquired 20 min after an intravenous bolus injection of 0.2 mmol/kg gadobutrol (Gadovist, BayerShering, Germany) in a 3-Tesla LGE-CMR scanner (Magnetom Trio, Siemens Healthcare, Germany) using a 3D free-breathing navigator and an ECG-gated inversion recovery gradient-echo sequence applied in axial orientation. Voxel size was 1.25x1.25x2.5 mm.

Image post-processing and LA segmentation

LGE-CMR studies with poor image quality or artifacts were excluded from the analysis. Left atrial (LA) wall was segmented using the ADAS® image post-processing software (Galgo Medical, Barcelona, Spain). Epicardial and endocardial LA wall contours were manually drawn in each axial plane. To minimize endocardial and epicardial segmentation artifacts, ADAS constructed a mid-myocardial (50% thickness) layer and

built a 3D shell that could be edited to ensure that it crossed through the wall (Figure 1A). PV at their ostia and the mitral valve were excluded from fibrosis analysis. Pixel signal intensity maps were obtained. Image intensity ratio (IIR) was calculated as the ratio between the signal intensity of each pixel and the mean LA blood pool intensity.[9] IIR values were color coded (fibrosis in red) and projected into the 3D LA shell (Figure 1B). IIR >1.20 were considered fibrosis, following an study on healthy volunteers, as previously reported by our group. [13] A detailed description of image post-processing is described in Supplemental material.

Regional fibrosis analysis

Using a methodology that semi-automatically divides the atrium into anatomically meaningful regions, the presence or absence of fibrosis was analyzed regionally in the 3D LA shell. Briefly, we defined 12 segments in a LA mesh that serves as a template (Figure 1C), using the open source MeshLab software (Visual Computing Lab, Pisa, Italy). Then we transferred this parcellation from the template mesh to our LA post-processed shells, taking as reference the mitral valve and the PV (Figure 2). After excluding PV, LA appendage, and mitral valve, 12 segments were established in the atrial wall:

- Segments 1-4, posterior wall. The boundaries of this area are the line between the superior edge of the ostium of superior pulmonary veins, the line that joins inferior and superior ostia of homolateral PV, and the line that joins the inferior edge of inferior PV.
- Segment 5 (left) and 6 (right), floor. The boundaries of these two equal-sized regions are the inferior posterior wall and the posterior aspect of the mitral annulus.
- Segment 7, interatrial septal wall.

- Segments 8-11, anterior wall. The boundaries are the high posterior wall and the anterior aspect of the mitral annulus and the LA appendage, excluded from fibrosis analysis due to high probability of technical errors in segmentation (Mitral valve is *per se* an area of hyperenhancement and LA appendage morphology makes it dificult to assure to be delineating the atrial wall).
- Segment 12, left lateral wall. The boundaries are the anterior wall and the left floor (Segment 5); it includes the base of the LA appendage and part of the mitral isthmus region.

For each region, the percentage of fibrosis was calculated as the fibrotic area (IIR>1.20) divided by total area. Further, we qualitatively recorded the presence or absence of fibrosis. Presence of fibrosis was considered when more than 2.5% of each segment was involved. Although any cut-off for existence of fibrosis is arbitrary and fibrosis means a continuum of severity, 2.5% represents the mean fibrosis observed at this threshold in a healthy population. [13]

Statistical analysis

Continuous variables are presented as mean ± standard deviation and compared with a t-test/Mann–Whitney test or one-way analysis of variance (ANOVA)/Kruskal–Wallis test. Categorical variables are summarized as total number (and percentage) and compared with a Chi-square test. To compare regional fibrosis percentages between segments, we used one-way ANOVA adjusted by contrast multiplicity according to Bonferroni post-hoc strategy. Linear correlation was used for correlations between LA fibrosis and continuous variables. Intra and inter-observer concordance was analyzed using the Lin correlation coefficient.

All analyses were performed using SPSS software for Windows, version 18.0 (Chicago, IL, USA). A p-value of 0.05 was considered statistically significant.

RESULTS

The LGE- CMR images were evaluated by two expert operators (EM,NC) and after exclusions for poor quality, inadequate inversion time and artifacts, images from 76 (68%) patients (mean age, [55±10] years; 61 [80.3%] men) were considered for processing and analysis. Baseline characteristics, including prevalence of hypertension, diabetes, and structural heart disease, are shown in Table 1. In 53.9% of the cases the arrhythmia was paroxysmal.

Mean CHA_2DS_2-VASc was 1.13. Other mean values of interest were LA anteroposterior diameter, as assessed by transthoracic echocardiogram in paraesternal long-axis view, 42.5±5.3 mm; volume, 96.8±29.6 ml; LA sphericity, 79.1±3.2; percentage of atrial wall fibrosis in all patients, 8.48±8.6% (excluding PV, LA appendage, and mitral valve).

Regional fibrosis analysis

The percentage of patients showing significant atrial fibrosis was 81.6%. Presence of fibrosis was defined as positive when it was visualized in more than 2.5% of global atrium surface based in the threshold in our previous study.[13] Patients with fibrosis were more often men (83.7% vs 74.1% NS) had a mean age of 55.48 (vs 54.76 NS), and a higher proportion of persistent AF type (53.1% Vs 33.3% p=0.07), compared to patients without fibrosis.

The regional analysis of fibrosis in these patients showed that native fibrosis was not uniformly distributed along the LA wall (Table 2). Globally, the posterior wall and floor areas were more affected by fibrosis, with 17.49% ± 14.06 and 14.38% ±13.83, respectively.

Posterior wall segments 3 and 5, corresponding to the area close to the left inferior PV, had significantly more fibrosis, compared to all other segments (40.42%±23.96 and

25.82%±21.24, respectively; p<0.001). Segments 8 and 10 in the anterior area contained the lowest proportion of fibrosis (2.54%±5.78 and 3.82%±11.59, respectively; p<0.001) (Figure 3). A detailed bonferroni post-hoc analysis of multiple comparisons is described in supplemental table 1.

The intra and inter-observer Lin concordance correlation coefficients for global fibrosis percentage were 0.99 and 0.97, respectively.

Atrial fibrosis predictors

Age >60 years was the only clinical characteristic associated with increased percentage of LA fibrosis (95%CI 0.19% to 8.39%, p=0.04). Persistent AF showed a trend toward association with increased fibrosis (95%CI -0.19% to 7.83%, p=0.08). In our population, there was no association between fibrosis and other clinical and echocardiographic characteristics such as hypertension, diabetes, AF duration, LA volume, sphericity or ejection fraction. This results are detailed in supplemental table 2.

DISCUSSION

The present study in patients with AF showed a preferential distribution of fibrosis detected by LGE-CMR around the posterior wall surrounding the ostium of the left inferior PV, compared to other LA locations. Age >60 years was the only clinical characteristic associated with higher percentage of fibrosis at this site, although persistent AF showed a trend toward this association.

Native regional atrial fibrosis: Histological assessment

Histological studies of the location and characterization of atrial fibrosis in humans are scarce. The analysis has been limited to areas in which samples can be collected from cardiac biopsy. Corradi et al [7] compared the percentage of fibrosis in two LA regions of 33 patients referred for surgery due to chronic AF associated with mitral disease and 16 autoptic controls. The area of the LA wall around the PV showed more interstitial

fibrosis than the wall of the LA appendage. Platonov et al [14] analyzed 30 specimens from 5 atrial locations (superior PV, inferior PV, center of posterior left atrial wall, terminal crest and Bachmann's bundle), collected during autopsies of patients with nonvalvular permanent AF, paroxysmal AF, and without AF history. They reported a higher percentage of fibrosis in the posterior wall and left inferior PV samples, but the differences were not significant. Nonetheless, the observation of more prominent fibrosis around the posterior wall adjacent to the left inferior PV in patients with limited atrial remodeling is intriguing, and has no obvious explanation. It could be interesting to analyze fibrosis at this location, which is anatomically close to the descending aorta, in experimental models. Permanent trauma caused by the impact of the aortic pulse on the atrial wall may potentially play a role in this fibrosis. Further studies are needed to explore this observation in depth.

Native regional atrial fibrosis: LGE-CMR assessment

Identification of the severity and location of fibrosis may be influenced by the methodology employed. Several groups have proposed algorithms to identify fibrosis at the atrial level in patients with AF [8, 9, 13, 15]. We did not find relevant differences in CMR acquistion protocols between groups that would give rise to substantial variances in fibrosis visualization. Discrepancies in total fibrosis amount and localization are determined by image post-processing and threshold of normality. The method described by Oakes et al [8] uses a variable threshold ranging from 2 to 4 standard deviations above the mean for healthy myocardium intensity established by expert opinion making reproducibility difficult. This method could overestimate fibrosis for example, identifying a mean of 18.1% of pathological tissue in a cohort of atrial fibrillation patients,[10] a higher percentage than was observed in the present study, although their patients may have had more severe atrial disease. Contrary to our results,

the lateral wall was the most affected segment in the cited study, followed by the posterior wall, and the post-hoc analysis of regional fibrosis in their population also showed a high percentage of fibrosis on the anterior wall. [16] These variations in fibrosis location could be explained by a less restrictive threshold that would increase the amount of fibrosis equally throughout all the atrium. Using the same algorithm for fibrosis detection in a general population of cardiology patients, Cochet et al reported , a mean of fibrosis of 18.4 ± 8.9% of the LA wall. They observed that fibrosis was predominantly located at posterior wall irrespective of previous diagnosis of AF. [17]. In this case and using the same Utah methodology, the lateral wall was the least affected segment.

Taking a different approach, Khurram et al. proposed a normalized signal IIR method to enable a more objective comparison between individuals. [9] Although this is the same standardization we use, in their study, the threshold in patients with AF is based on the correlation between IIR and bipolar voltage maps obtained before an ablation procedure, defining IIR <0.97 as the cut-off for pathological native tissue. This threshold probably has higher sensitivity to detect fibrosis, at the cost of lower specificity, compared to the normalized IIR <1.20 calculated by our group, which was derived from a cohort of healthy young volunteers. [13] The mean LA LGE extent in their population was 14.1 ± 10.4%, significantly greater than in ours. Using the 0.97 threshold, Fukumoto et al. [18] have also reported a good correlation between IIR and local conduction velocity, especially in patients with persistent AF. Although they make no reference to the different detailed locations of fibrosis, the most affected areas they observed are adjacent to the left PV antra (the septo-pulmonary bundle region), [18] corresponding with segments 1, 3 and 5 in our study. In fact, these areas correspond to

a change in direction and thickness of fibers coming from the septo-pulmonary bundle that could make it more susceptible to remodeling

On the other hand, in disagreement with our results, the study of Rolf et al [19], analyzed the spatial distribution of low voltage areas (LVAs) in the electroanatomical mapping (sites of ≥3 adjacent low-voltage points <0.5 mV), involving the septum in 72% of cases, the anterior LA in 60%, the posterior wall in 51%, the atrial roof in 49%, and the inferior LA in 30%. Their study reported the presence of LVAs but not their extension.

Conditions associated with fibrosis

The risk factors that had previously been identified by LGE-CMR in cardiology patients are age, hypertension, history of cardiac disease, AF, and specifically persistent AF.[17] In our study, an older age was significantly associated with a higher amount of fibrosis, and persistent AF approached significance; both factors are known to be associated with more prominent remodeling. No patients in our series had long-standing persistent AF. The study by Hunter et al [20], contains a large proportion of long standing persistent AF. Peaks in atrial wall pressure stress were predominant around the ostia of the PVs which could explain why these areas are more affected by remodeling. In post-portem specimen~~t~~s, long-standing persistent AF has been associated with more extensive fibrosis at all locations. [14]

Limitations

Some limitations of our work must be acknowledged. First, LGE-CMR signal intensities are influenced by individual characteristics such as body mass index, renal function, and haematocrit, which might limit the validity of the algorithms used.

Second, small errors in technical and post-processing parameters may generate misinterpretations in the results. The accuracy of manual and semi-automated identification of the LA walls remains a critical aspect of image post-processing

protocols, largely depending on investigator experience. These errors were minimized by using a mid-myocardial layer (50% of atrial wall thickness) that prevents against mild inaccuracies in boundary segmentation and including only those studies adequate image quality (hence the high proportion [36%] of exclusions). Fibrosis analysis in LA appendage was also excluded because it was not considered sufficiently accurate in manual wall segmentation. Anatomical structures close to the atrial wall, especially regularly enhancing structures like the mitral valve and aortic wall, could determine some degree of artefact, which was taken into account in our segmentations and exclusions. Segmentations have been performed carefully in order to identify and delimit precisely the boundaries of the atrial wall in order to differentiate them from scar .

Finally, we used a restrictive threshold, IIR<1.20, to define the location of the most pathological tissue. Small changes in any threshold of a continuous variable might result in large changes in the percentage and location of fibrosis; nevertheless, our findings are consistent with histological effects as well as the low velocity conduction observed in another study.

Conclusion

The regional analysis of fibrosis assessed by LGE-CMR in a population of patients with AF showed a predominant distribution of the enhanced area at the atrium in the posterior wall and the floor adjacent to the antrum of the left inferior PV. The only clinical characteristic associated with a higher degree of fibrosis was age >60 years.

ACKNOWLEDGMENTS.

This work was partially supported by Fondo de Investigaciones Sanitarias-Instituto de Salud Carlos III (PI13/01747 and PI16/00435); Agencia de gestió d´Ajuts Universitaris I de Recerca (AGAUR) Exp: 2014_SGR_471; CERCA programme/Generalitat de

Catalunya; European Regional Development Fund (ERDF. European Union. A Way of Making Europe), the European Union's Horizon 2020 research and innovation programme under grant agreement No 633196 (CATCH ME), a grant by La MARATÓ-TV3 (Id. 20152730) and the Spanish Ministry of Economy and Competitiveness (DPI2015-71640-R).

The authors thank Mrs. Neus Portella for research assistance.

REFERENCES

[1] Wakili R, Voigt N, Kaab S, Dobrev D, Nattel S. Recent advances in the molecular pathophysiology of atrial fibrillation. *The Journal of clinical investigation* 2011; **121**: 2955-2968.

[2] Heijman J, Voigt N, Nattel S, Dobrev D. Cellular and molecular electrophysiology of atrial fibrillation initiation, maintenance, and progression. *Circulation research* 2014; **114**: 1483-1499.

[3] Xu J, Cui G, Esmailian F, Plunkett M, Marelli D, Ardehali A, et al. Atrial extracellular matrix remodeling and the maintenance of atrial fibrillation. *Circulation* 2004; **109**: 363-368.

[4] Fabritz L, Guasch E, Antoniades C, Bardinet I, Benninger G, Betts TR, et al. Expert consensus document: Defining the major health modifiers causing atrial fibrillation: a roadmap to underpin personalized prevention and treatment. *Nature reviews Cardiology* 2016; **13**: 230-237.

[5] Verheule S, Sato T, Everett Tt, Engle SK, Otten D, Rubart-von der Lohe M, et al. Increased vulnerability to atrial fibrillation in transgenic mice with selective atrial fibrosis caused by overexpression of TGF-beta1. *Circulation research* 2004; **94**: 1458-1465.

[6] Ausma J, Wijffels M, Thone F, Wouters L, Allessie M, Borgers M. Structural changes of atrial myocardium due to sustained atrial fibrillation in the goat. *Circulation* 1997; **96**: 3157-3163.

[7] Corradi D, Callegari S, Benussi S, Nascimbene S, Pastori P, Calvi S, et al. Regional left atrial interstitial remodeling in patients with chronic atrial fibrillation

undergoing mitral-valve surgery. *Virchows Archiv : an international journal of pathology* 2004; **445**: 498-505.

[8] Oakes RS, Badger TJ, Kholmovski EG, Akoum N, Burgon NS, Fish EN, et al. Detection and quantification of left atrial structural remodeling with delayed-enhancement magnetic resonance imaging in patients with atrial fibrillation. *Circulation* 2009; **119**: 1758-1767.

[9] Khurram IM, Beinart R, Zipunnikov V, Dewire J, Yarmohammadi H, Sasaki T, et al. Magnetic resonance image intensity ratio, a normalized measure to enable interpatient comparability of left atrial fibrosis. *Heart rhythm : the official journal of the Heart Rhythm Society* 2014; **11**: 85-92.

[10] Marrouche NF, Wilber D, Hindricks G, Jais P, Akoum N, Marchlinski F, et al. Association of atrial tissue fibrosis identified by delayed enhancement MRI and atrial fibrillation catheter ablation: the DECAAF study. *Jama* 2014; **311**: 498-506.

[11] Camm AJ, Lip GY, De Caterina R, Savelieva I, Atar D, Hohnloser SH, et al. 2012 focused update of the ESC Guidelines for the management of atrial fibrillation: an update of the 2010 ESC Guidelines for the management of atrial fibrillation. Developed with the special contribution of the European Heart Rhythm Association. *European heart journal* 2012; **33**: 2719-2747.

[12] Bisbal F, Guiu E, Cabanas-Grandio P, Berruezo A, Prat-Gonzalez S, Vidal B, et al. CMR-guided approach to localize and ablate gaps in repeat AF ablation procedure. *JACC Cardiovascular imaging* 2014; **7**: 653-663.

[13] Benito EM, Carlosena-Remirez A, Guasch E, Prat-Gonzalez S, Perea RJ, Figueras R, et al. Left atrial fibrosis quantification by late gadolinium-enhanced magnetic resonance: a new method to standardize the thresholds for reproducibility. Europace 2016; **26**: 473-80.

[14] Platonov PG, Mitrofanova LB, Orshanskaya V, Ho SY. Structural abnormalities in atrial walls are associated with presence and persistency of atrial fibrillation but not with age. *Journal of the American College of Cardiology* 2011; **58**: 2225-2232.

[15] Harrison JL, Jensen HK, Peel SA, Chiribiri A, Grondal AK, Bloch LO, et al. Cardiac magnetic resonance and electroanatomical mapping of acute and chronic atrial ablation injury: a histological validation study. *Eur Heart J* 2014; **35**: 1486-1495.

[16] Erik T Bieging AM, Joshua Cates, Nassir F Marrouche. Regional left atrial wall fibrosis and recurrence after atrial fibrillation ablation. *Journal of cardiovascular magnetic resonance : official journal of the Society for Cardiovascular Magnetic Resonance* 2016; **18**: P200.

[17] Cochet H, Mouries A, Nivet H, Sacher F, Derval N, Denis A, et al. Age, atrial fibrillation, and structural heart disease are the main determinants of left atrial fibrosis detected by delayed-enhanced magnetic resonance imaging in a general cardiology population. *Journal of cardiovascular electrophysiology* 2015; **26**: 484-492.

[18] Fukumoto K, Habibi M, Ipek EG, Zahid S, Khurram IM, Zimmerman SL, et al. Association of Left Atrial Local Conduction Velocity With Late Gadolinium Enhancement on Cardiac Magnetic Resonance in Patients With Atrial Fibrillation. *Circulation Arrhythmia and electrophysiology* 2016; **9**: e002897.

[19] Rolf S, Kircher S, Arya A, Eitel C, Sommer P, Richter S, et al. Tailored atrial substrate modification based on low-voltage areas in catheter ablation of atrial fibrillation. *Circulation Arrhythmia and electrophysiology* 2014; **7**: 825-833.

[20] Hunter RJ, Liu Y, Lu Y, Wang W, Schilling RJ. Left atrial wall stress distribution and its relationship to electrophysiologic remodeling in persistent atrial fibrillation. *Circulation Arrhythmia and electrophysiology* 2012; **5**: 351-360.

TABLE 1.

Baseline Characteristics of the population.

Demographics N: 76	
Age (years)	55 ±10
Men	61(80.3%)
Hypertension	43 (56.6%)
Diabetes mellitus	5 (6.6%)
OSA	9 (11.8%)
Structural heart disease	14 (18.4%)
$CHADsVASC_2$	1.13±1.19
Paroxysmal AF	41 (53.9%)
Echocardiography and CMR data	
TTE LA anteroposterior diameter (mm)	42 ±5
TTE Left ventricular ejection fraction (%)	58 ±7
CMR LA Area (cm2)	28.89±5.97
CMR LA Volume (cm3)	96.8±29.6
LA sphericity (LASP)	79.10±3.22
Fibrosis-CMR-LGE (%)	8.48 (±) 8.69

(AF: atrial fibrillation; CMR: Cardiac Magnetic Resonance; LA: left atrial; LASP: left atrial sphericity; OSA: obstructive sleep apnea; TTE: transthoracic echocardiogram)

TABLE 2.

Regional fibrosis quantification. Posterior wall (1-4 segments); floor (5-6 segments); septal wall (segment 7); anterior wall (8-11 segments); left lateral wall (segment 12).

REGIONS GROUPED	% FIBROSIS†	P	REGION	PRESENCE of FIBROSIS	P	% FIBROSIS*	P
ALL ATRIUM	10.19 ± 8.75	<0.001		81.6%	<0.001		<0.001
POSTERIOR WALL	17.49± 14.06		1	61.8%		16.84 ± 17.22	
			2	50%		8.80 ± 12.80	
			3	85.5%		40.42 ± 23.96	
			4	55.3%		13.94 ± 20.27	
FLOOR	14.38 ± 13.83		5	77.6%		25.82 ± 21.24	
			6	42.1%		7.33 ± 12.57	
SEPTAL WALL	4.14 ± 6.58		7	35.5%		4.14 ± 6.58	
ANTERIOR WALL	3.58 ± 7.41		8	18.4%		2.54 ± 5.78	
			9	23.7%		4.46 ± 10.02	
			10	21.1.5%		3.82 ± 11.59	
			11	25%		4.13 ± 9.33	
LEFT LATERAL WALL	11.83 ± 13.92		12	52.6%		11.83 ± 13.92	

(† mean percentage excluded patients without fibrosis)

FIGURE LEGENDS

FIGURE 1. Cardiac Magnetic Resonance segmentation and left atrium regional parcellation. Figure 1A corresponds with the original LGE sequence showing areas with hyper-enhancement. The wall is manually drawn by the operator. Based on previously determined thresholds, a 3-dimensional color-coded shell is constructed (Figure 1B) by ADAS software (fibrosis in red). Figure 1C shows the division of an arbitrary LA in the 12 proposed regions.

FIGURE 2. Regional Fibrosis Analysis. The LA division defined in the template mesh is transferred to the 3-dimesnsional post-processed shell (A), allowing the regional quantification of fibrosis (B).

FIGURE 3 Regional distribution of left atrial fibrosis. Bars represente mean percentage of fibrosis +1SD Colors appoint the different agrouped areas. Bars represent +1SD. (* segments with significant higher fibrosis)

1 FIGURE 1.

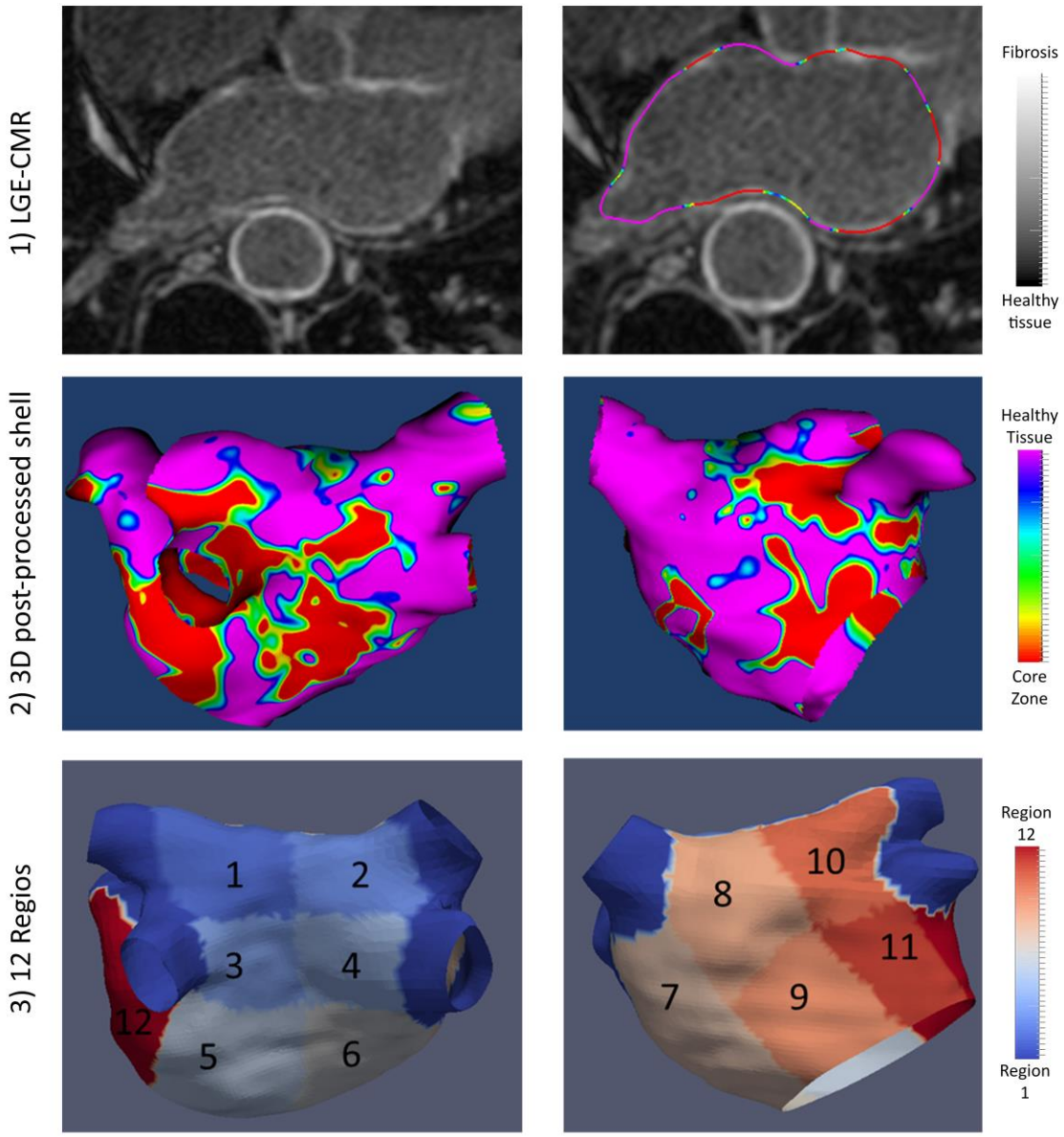
1) LGE-CMR
Fibrosis
Healthy tissue
2) 3D post-processed shell
Healthy Tissue
Core Zone
3) 12 Regios
1
2
3
4
5
6
12
7
8
9
10
11
Region 12
Region 1

2

3

1 FIGURE 2.

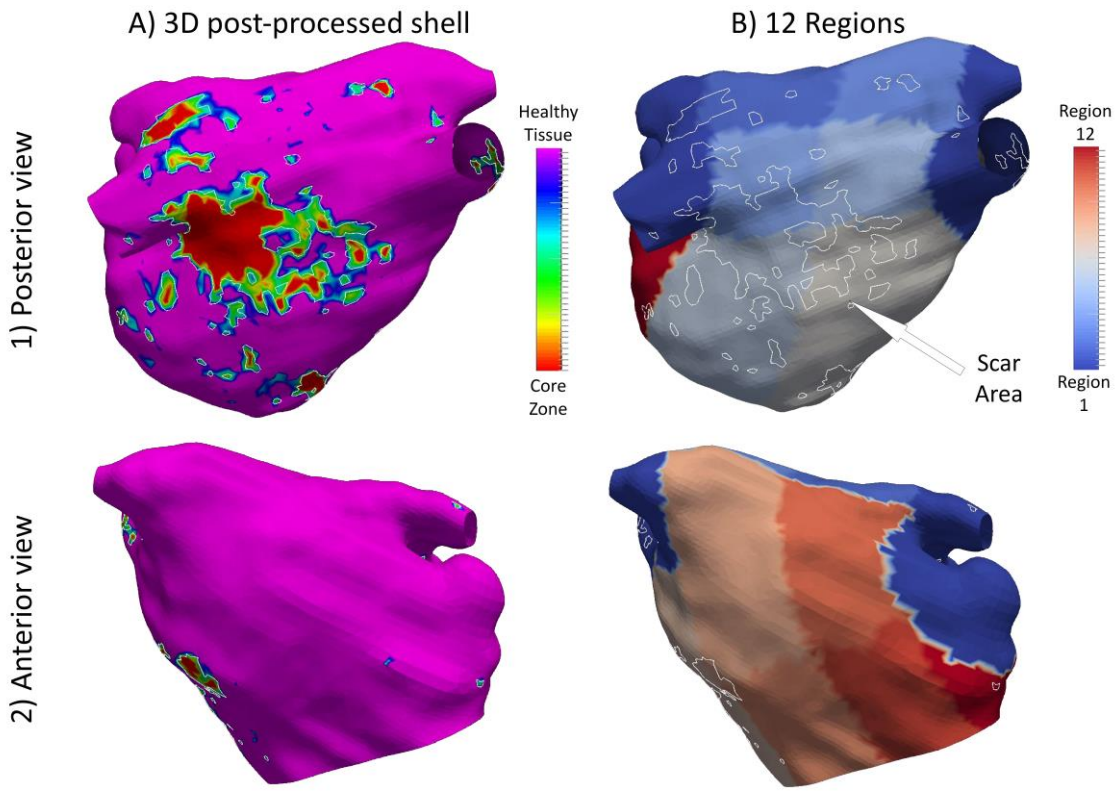
A) 3D post-processed shell
B) 12 Regions
1) Posterior view
2) Anterior view
Healthy Tissue
Core Zone
Region 12
Region 1
Scar Area

2
3

1 FIGURE 3.

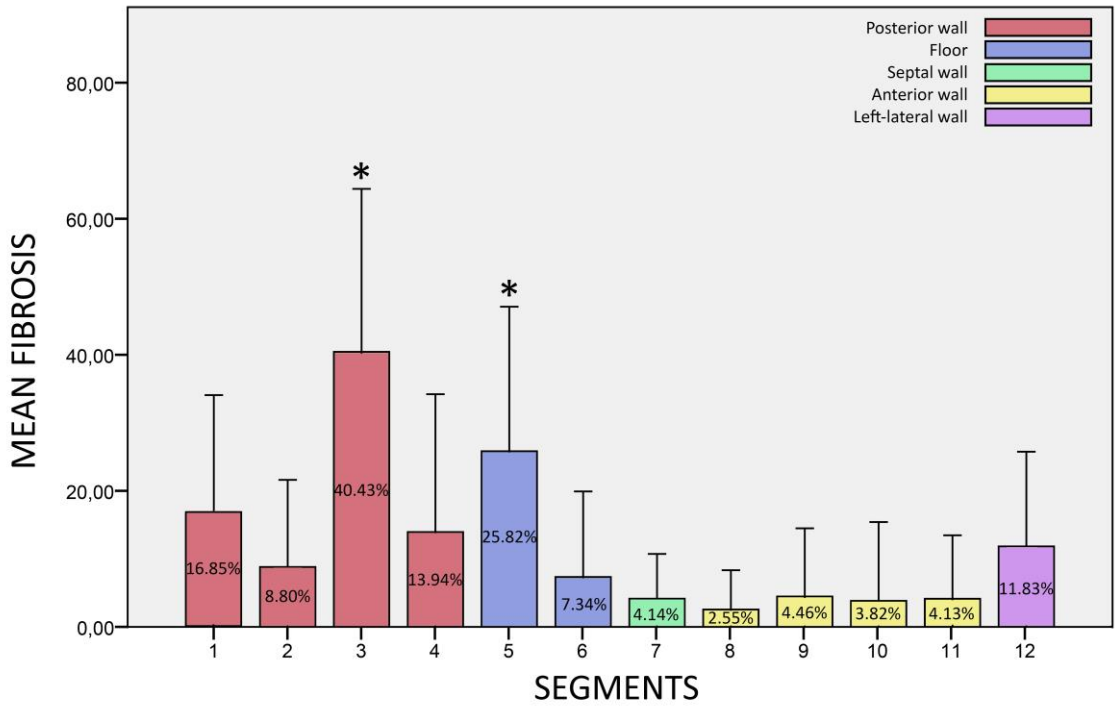
Posterior wall
Floor
Septal wall
Anterior wall
Left-lateral wall
MEAN FIBROSIS
80,00
60,00
40,00
20,00
0,00
*
*
16.85%
8.80%
40.43%
13.94%
25.82%
7.34%
4.14%
2.55%
4.46%
3.82%
4.13%
11.83%
1
2
3
4
5
6
7
8
9
10
11
12
SEGMENTS

2

Representative Figure

Click here to download Representative Figure
Representative_figure.jpg

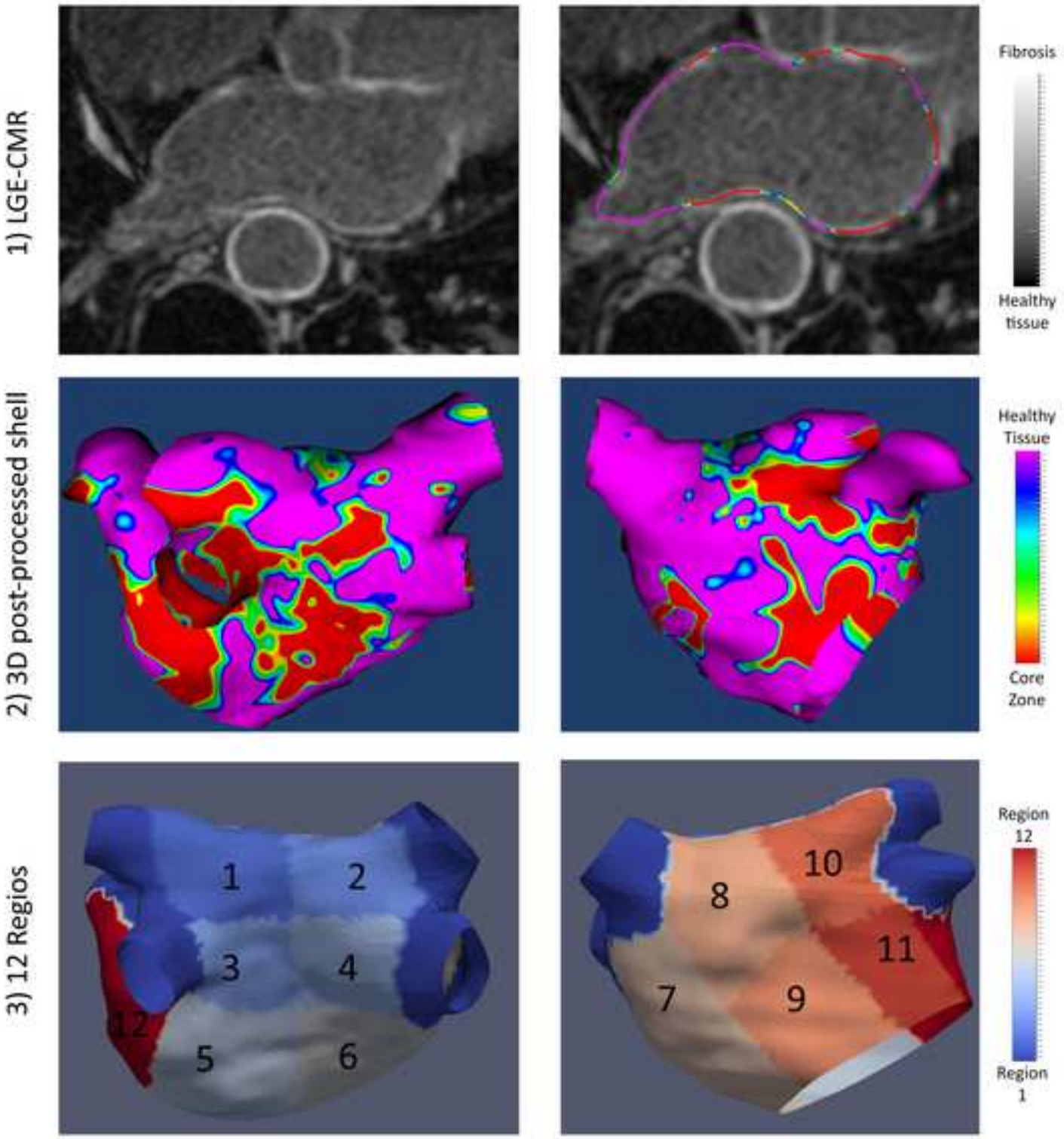

Figure

Click here to download Figure Figure_1.jpg

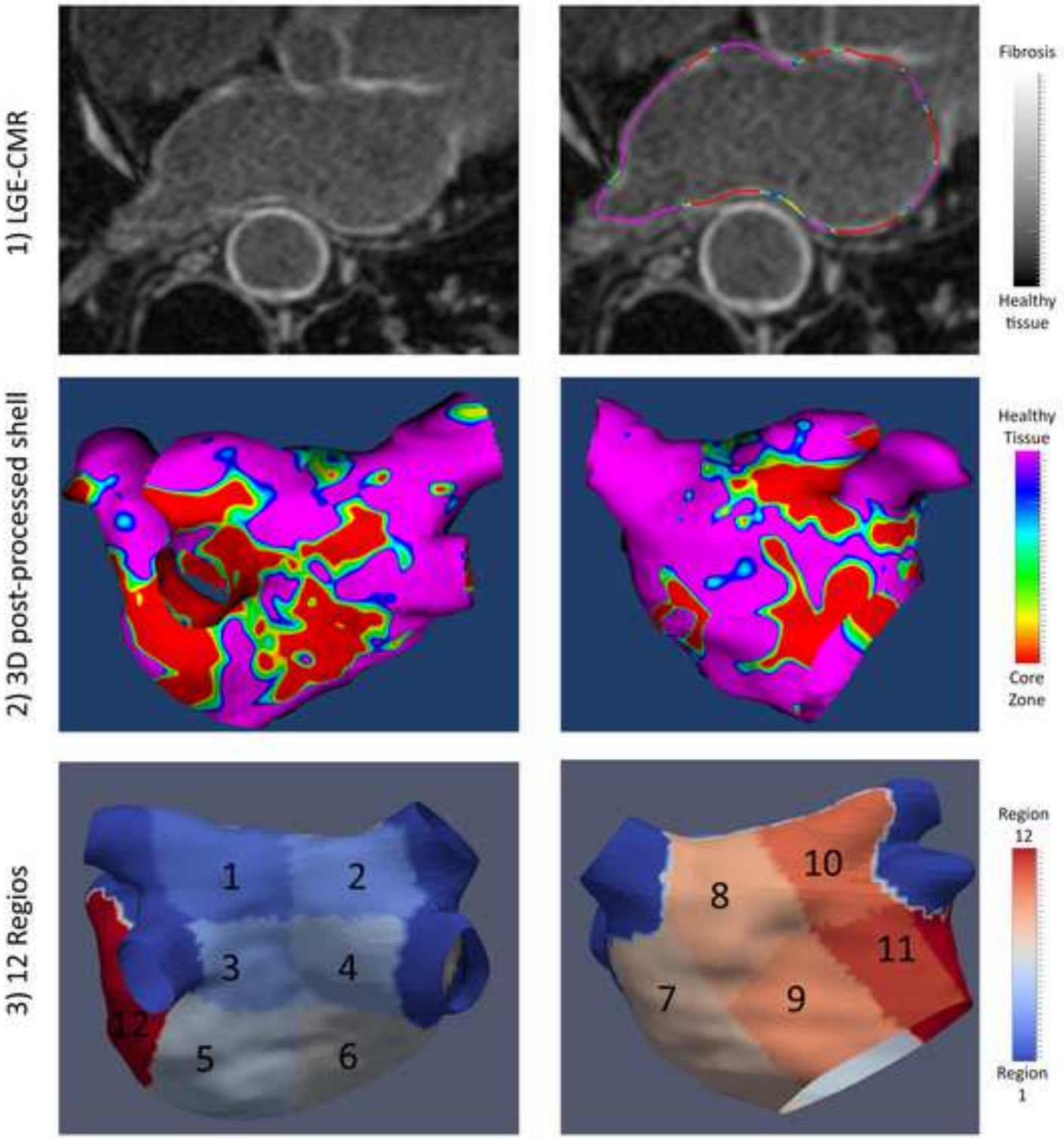

Figure

Click here to download Figure Figure_2.jpg

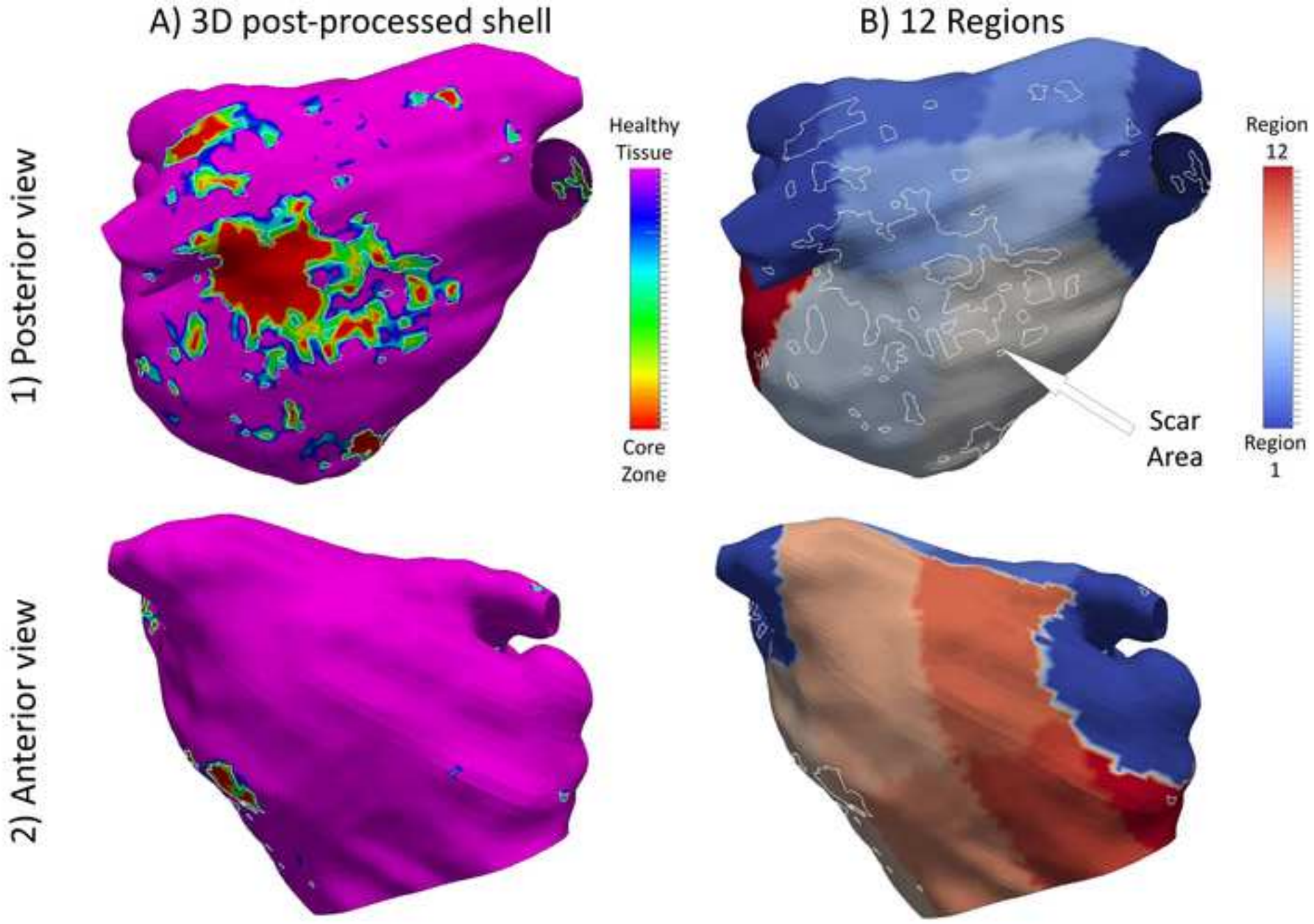

Figure

Click here to download Figure Figure_3.jpg

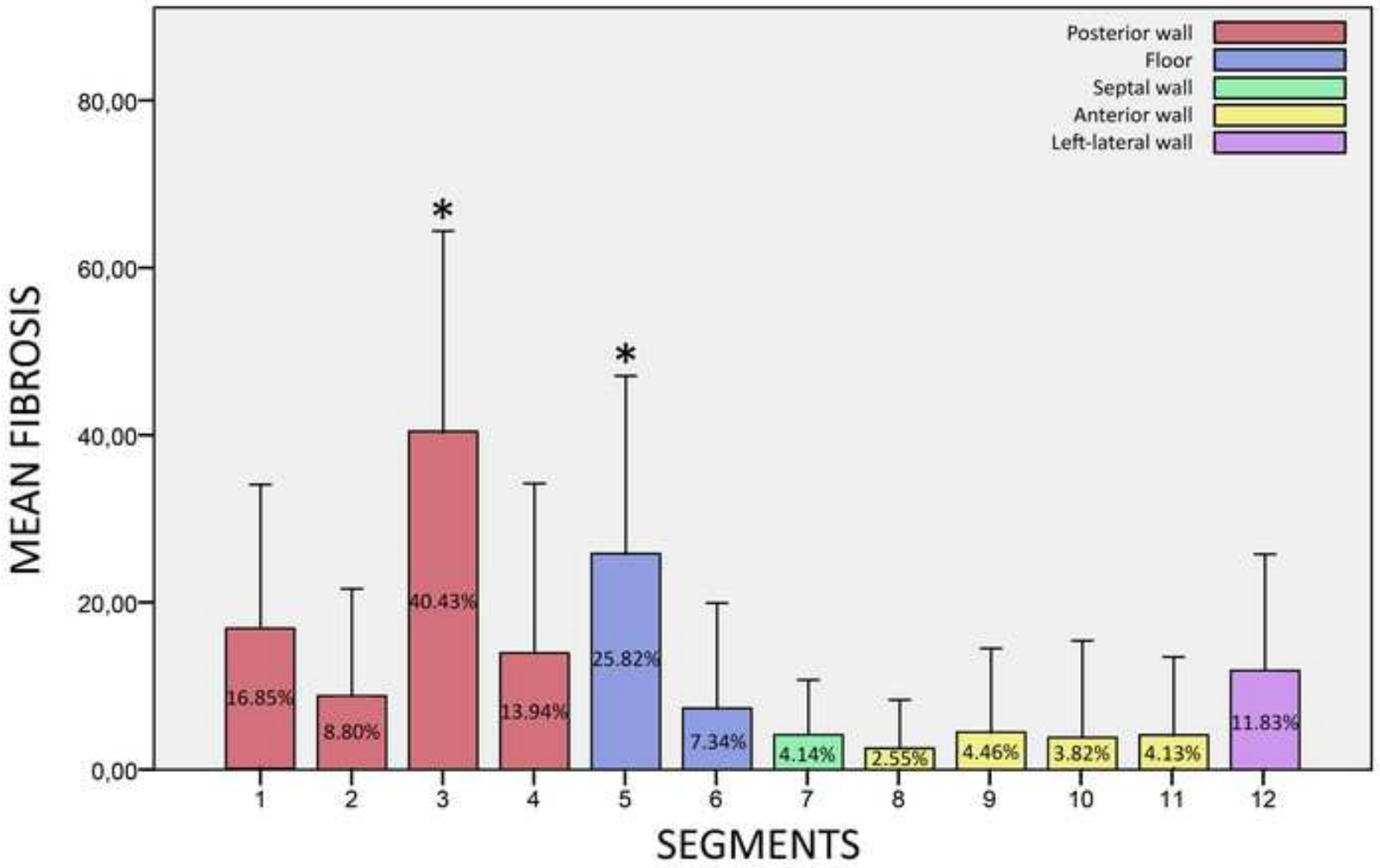

Table

TABLE 1.

Baseline Characteristics of the population.

Demographics N: 76	
Age (years)	55 ±10
Men	61(80.3%)
Hypertension	43 (56.6%)
Diabetes mellitus	5 (6.6%)
OSA	9 (11.8%)
Structural heart disease	14 (18.4%)
$CHADsVASC_2$	1.13±1.19
Paroxysmal AF	41 (53.9%)
Echocardiography and CMR data	
TTE LA anteroposterior diameter (mm)	42 ±5
TTE Left ventricular ejection fraction (%)	58 ±7
CMR LA Area (cm2)	28.89±5.97
CMR LA Volume (cm3)	96.8±29.6
LA sphericity (LASP)	79.10±3.22
Fibrosis-CMR-LGE (%)	8.48 (±) 8.69

(AF: atrial fibrillation; CMR: Cardiac Magnetic Resonance; LA: left atrial; LASP: left atrial sphericity; OSA: obstructive sleep apnea; TTE: transthoracic echocardiogram)

Table

TABLE 2.

Regional fibrosis quantification. Posterior wall (1-4 segments); floor (5-6 segments); septal wall (segment 7); anterior wall (8-11 segments); left lateral wall (segment 12).

REGIONS GROUPED	% FIBROSIS†	P	REGION	PRESENCE of FIBROSIS	P	% FIBROSIS*	P
ALL ATRIUM	10.19 ± 8.75	<0.001		81.6%	<0.001		<0.001
POSTERIOR WALL	17.49± 14.06		1	61.8%		16.84 ± 17.22	
			2	50%		8.80 ± 12.80	
			3	85.5%		40.42 ± 23.96	
			4	55.3%		13.94 ± 20.27	
FLOOR	14.38 ± 13.83		5	77.6%		25.82 ± 21.24	
			6	42.1%		7.33 ± 12.57	
SEPTAL WALL	4.14 ± 6.58		7	35.5%		4.14 ± 6.58	
ANTERIOR WALL	3.58 ± 7.41		8	18.4%		2.54 ± 5.78	
			9	23.7%		4.46 ± 10.02	
			10	21.1.5%		3.82 ± 11.59	
			11	25%		4.13 ± 9.33	
LEFT LATERAL WALL	11.83 ± 13.92		12	52.6%		11.83 ± 13.92	

(† mean percentage excluded patients without fibrosis)